


Article

Operational Modal Analysis and Safety Assessment of a Historical Masonry Bell Tower

Corrado Chisari ^{1,*} , Mattia Zizi ¹ , Angelo Lavino ¹, Salvatore Freda ² and Gianfranco De Matteis ¹ 

¹ Department of Architecture and Industrial Design, University of Campania “Luigi Vanvitelli”, 81031 Aversa, CE, Italy; mattia.zizi@unicampania.it (M.Z.); angelo.lavino@unicampania.it (A.L.); gianfranco.dematteis@unicampania.it (G.D.M.)

² Diocesan Office for Ecclesiastical Cultural Heritage and Religious Buildings, Diocese of Sessa Aurunca, 81037 Sessa Aurunca, CE, Italy

* Correspondence: corrado.chisari@unicampania.it

Abstract: The seismic assessment of historical masonry bell towers is of significant interest, particularly in Italy, due to their widespread presence and inherent vulnerability given by their slenderness. According to technical codes and standard practice, the seismic evaluation of masonry bell towers can be conducted using a range of methodologies that vary in their level of detail. This paper presents a case study of a historical masonry bell tower located in the Caserta Province (Italy). Extensive investigative efforts were undertaken to determine the tower’s key geometric and structural characteristics, as well as to document ongoing damage phenomena. The dynamic behavior of the tower was assessed through ambient vibration testing, which enabled the identification of the principal modal shapes and corresponding frequencies, also highlighting peculiar dynamical characteristics caused by the damage conditions. Subsequently, the seismic assessment was carried out using both Level 1 (simplified mechanical) and Level 2 (kinematic limit analysis) methodologies. This assessment helped identify the most probable collapse mechanisms and laid the foundation for employing more advanced methodologies to design necessary retrofitting interventions. The study emphasizes the importance of Level 2 analyses for structures where out-of-plane failure mechanisms are likely due to pre-existing cracking. Both approaches provide less-than-unity acceleration factors, ranging from 0.45 for Level 1 (assuming non-ductile behavior) to 0.59 for Level 2, in this case specifically using the information available about existing cracking pattern.

Keywords: ambient vibration testing; limit analysis; kinematic approach; material testing; geometrical survey; cultural heritage



Citation: Chisari, C.; Zizi, M.; Lavino, A.; Freda, S.; De Matteis, G.

Operational Modal Analysis and Safety Assessment of a Historical Masonry Bell Tower. *Appl. Sci.* **2024**, *14*, 10604. <https://doi.org/10.3390/app142210604>

Academic Editors: Konstantinos Morfidis and Konstantinos Kostinakis

Received: 4 October 2024

Revised: 28 October 2024

Accepted: 1 November 2024

Published: 17 November 2024



Copyright: © 2024 by the authors. Licensee MDPI, Basel, Switzerland. This article is an open access article distributed under the terms and conditions of the Creative Commons Attribution (CC BY) license (<https://creativecommons.org/licenses/by/4.0/>).

1. Introduction

Italy, renowned for its rich cultural heritage, is home to an extraordinary number of historical bell towers, built over the past centuries and predominantly constructed from masonry, and often so important as to shape the country’s identity and landscape.

The historical importance of these bell towers cannot be overstated. Many of them date back to medieval times, representing the architectural style and construction techniques of their respective eras. They were often built to signify the presence of a church or a cathedral, serving both religious and communal purposes. Over the centuries, these bell towers have witnessed several historical events and have become integral parts of their communities. However, their historical and cultural significance is juxtaposed with their structural and seismic vulnerabilities, particularly during seismic events.

Past seismic events provide valuable insights into the behavior of masonry bell towers under earthquake loading. Reconnaissance performed on masonry churches in the aftermath of the last Italian earthquakes (e.g., L’Aquila 2009, Emilia-Romagna 2012 and Central Italy 2016–2017) testified that bell towers may experience severe damage during seismic events [1,2].

Historical records and modern case studies of seismic damage to these structures reveal common patterns of failure and highlight the most vulnerable aspects of their design and construction. For this reason, similarly to churches [3], and as suggested in Ministerial Italian Guidelines for Cultural Heritage [4], the seismic assessment of masonry bell towers can be performed at different evaluation Levels (ELs), from simplified mechanical approaches (EL1) to more accurate and sophisticated analyses (EL2, EL3).

In particular, according to EL1 [5–7], the tower is represented as a variable-cross-section vertical beam subjected to lateral forces simulating seismic forces. A simplified yet realistic representation of the plan view at each floor is required, along with the definition of a very limited number of homogeneous material properties (compression strength). EL2 [5,7–10] needs an accurate geometric representation of the bell tower and the vulnerability estimate is given by the results of analyses at collapse, which are performed for the most representative mechanisms. Finally, EL3 [5,7,11–15] is based on accurate numerical modeling of the structure, requiring detailed surveying, material characterization and geometrical representation. Although it is not included in the Italian Guidelines, the existence of a lower-detailed level EL0 should be also mentioned [16–18]. Such methodologies, in which the bell tower is identified by very few typological parameters, allow for defining a vulnerability ranking rather than an estimate of safety.

It is clear that the evaluation level selected for a specific case primarily depends on two key factors: the available information regarding the structure and the objective of the analysis (with global interventions requiring an EL3 assessment). However, the reliability of these methodologies should also be linked to the actual behavior of the structure under investigation, including any degradation or cracking phenomena. The use of more detailed levels of assessment is not always the optimal solution, particularly when significant uncertainties are associated with mechanical properties and strength parameters in numerical models.

In the present study, a case study of the bell tower of St. Lucia Church in Cellole (Caserta Province) is addressed. Based on wide preliminary investigation activity, including a geometrical survey, tests on materials and dynamical characterization, the main structural features of the tower were identified. Given the presence of a significant cracking pattern, the assessment of the tower was performed by adopting EL1 and EL2 methodologies for in-plane and out-of-plane collapse modes, respectively. The final results are provided in terms of acceleration factors, and the paper as a whole aims at showing the complex and multifaceted methodology involved in the structural analysis and vulnerability assessment of material Cultural Heritage.

2. The Case Study: The Bell Tower of the St. Lucia Church in Cellole (CE)

2.1. Geometrical Survey

The structure under investigation (Figure 1) is the bell tower of the Church of St. Lucia in Cellole (Caserta Province, Italy). The tower is adjacent to the homonymous church, with which shares the ground floor rooms.

A complete laser-scanner 3d survey of the church and the tower was performed in order to define the main geometrical characteristics. The instrument was Leica BLK360 Imaging Laser Scanner (Wetzlar, Germany), while the raw data were then processed by Cyclone Registrar 360 software. The whole complex including the church and the bell tower was shot from 60 points. In Figure 2 the global view of the 3d laser scanner survey is shown.

The tower has a rectangular base and can be geometrically divided into five sectors. The first sector extends vertically to approximately 5.30 m, with external dimensions of 4.75×3.80 m. The second and third sectors have the same external dimensions as the first one, but with slightly chamfered corners on the southern side. Both sectors have a vertical extension of about 3.50 m, while the fourth sector (constituting the belfry of the tower) is 2.80 m high, with a smaller in-plane dimension of 3 m. The final sector is a reduced

extension of the tower, approximately 2.40 m high, probably added at a later time, and also presents an external bell.

In plan, the tower can be divided into two parts along its major dimension throughout its height. Specifically, it features a transversal wall that defines two sections: a cave-like section on the southern side and a complex system of flying buttresses that support an internal staircase, allowing access from the ground level to the top sector.

The complete geometrical survey of the tower, including the plan views at the different sectors and two sections, is provided in Figure 3.

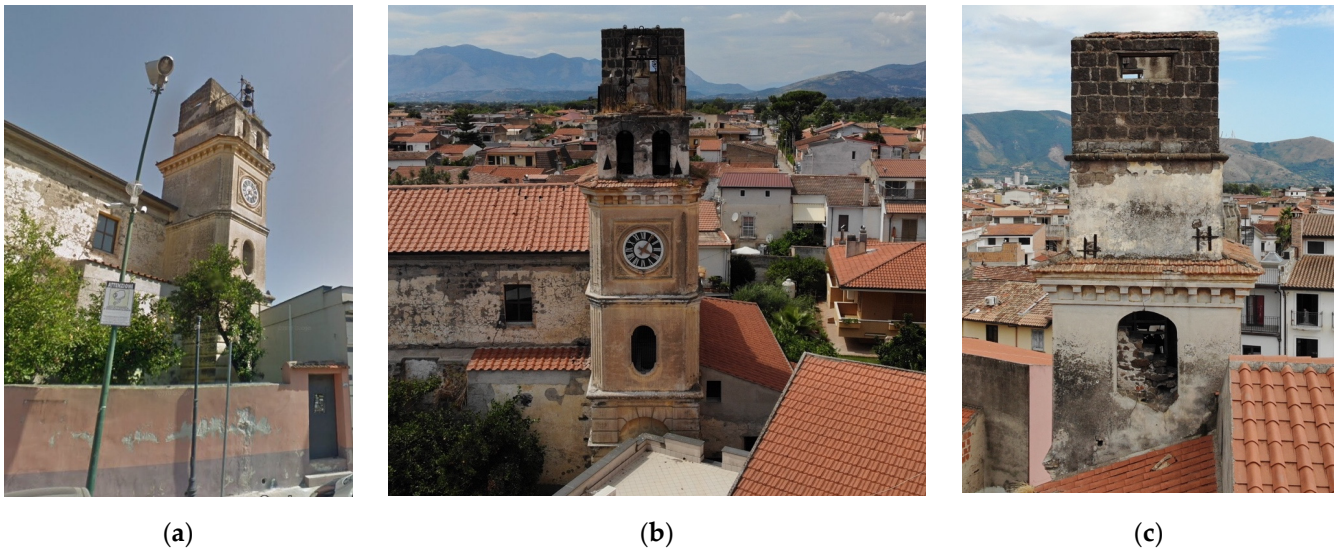


Figure 1. The tower of the St. Lucia Church in Cellole (CE): (a) south-west, (b) south and (c) north views.



Figure 2. Global view of the 3D laser scanner survey.

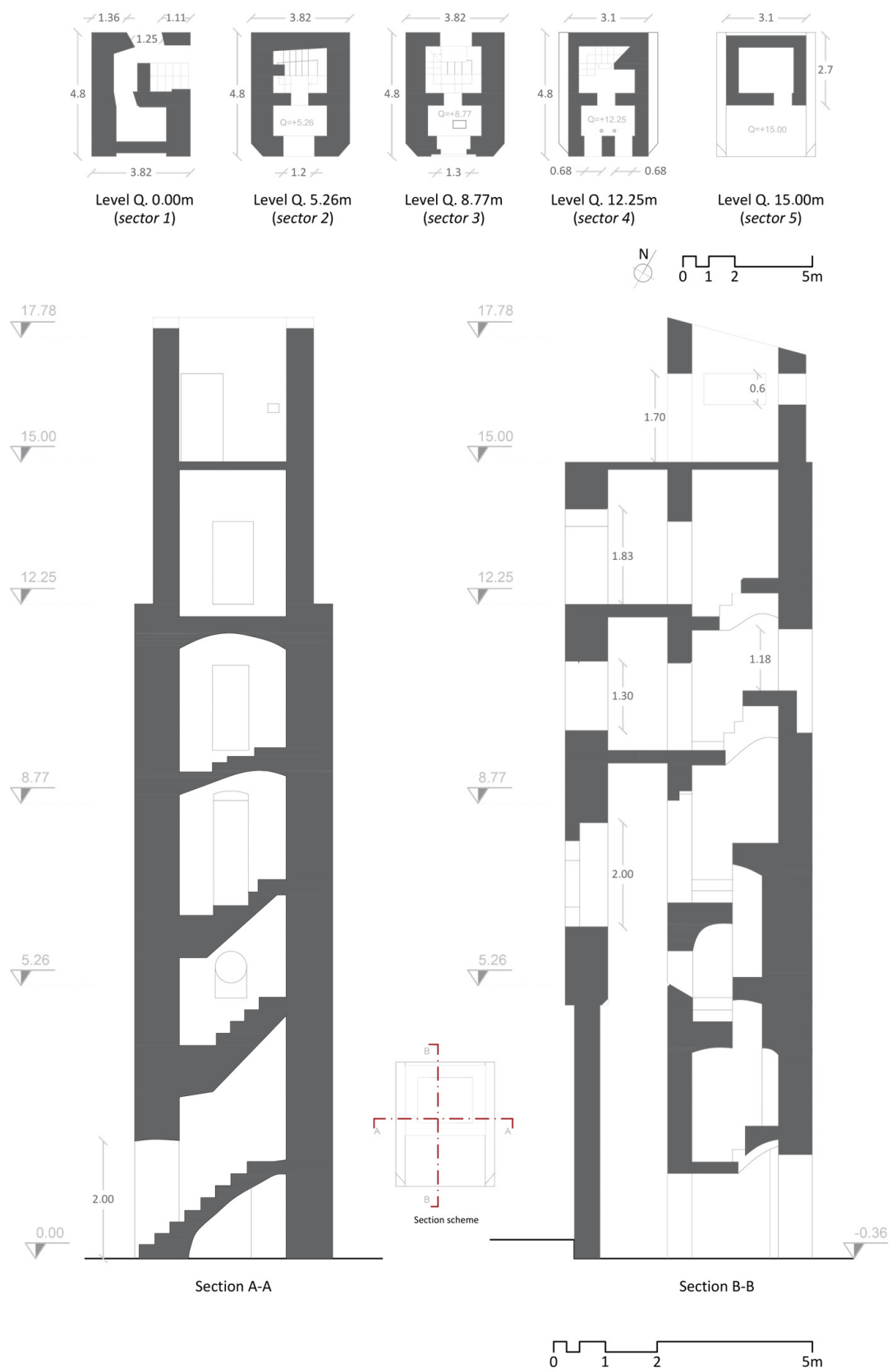


Figure 3. Geometrical survey of the tower of St. Lucia Church in Cellole (CE).

2.2. Structural Features, Material Characteristics and State of Conservation

To define the main structural features of the tower and to mechanically characterize the existing materials, a series of non-destructive and minimally destructive tests were conducted. The material used for the construction of the tower is gray tuff masonry, a soft volcanic stone typical of this geographical area. Its compressive strength is generally quite low compared to other stones and materials (e.g., clay bricks) used across the Italian peninsula for masonry structures. This condition was confirmed by sclerometer tests performed on the masonry units, which returned an average compressive strength of 0.7 MPa.

The quality of mortar, particularly its compressive strength, was also assessed through non-invasive tests (i.e., penetrometer). The instrument used had a lower threshold of admissible strength range of 0.4 MPa. All tests returned strength values below this threshold, indicating very poor mortar quality.

The bad quality of masonry was confirmed by compressive tests on tuff samples and double flat jack tests, which returned compressive strengths of 0.86 MPa and 0.65 MPa, respectively.

Beyond the mechanical characteristics of the existing material, the tower is in a poor state of conservation, with visible signs of degradation and cracking. Specifically, the visual inspection revealed that many of the squared gray tuff blocks showed signs of detachment, especially around the openings. In the bell chamber, many blocks appeared displaced, disconnected and infested with weeds due to the disrepair affecting the structure. The natural deterioration of the masonry, plaster and roof, combined with lack of maintenance, has resulted in a structure with serious conservation and stability issues.

Furthermore, significant vertical cracking was observed on the east and west façades, affecting the external walls of the second, third and fourth levels. The presence of cracks on the west façade was clearly confirmed through thermographic inspections conducted on-site from the ground level and with the support of a drone (Figure 4). On the other hand, the situation was even more severe on the opposite wall (east façade), where the cracks were visible to the naked eye and further confirmed by thermal imaging (Figure 5). The presence of these vertical cracks may be connected to the configuration of the last sector, whose construction clearly took place in a latter phase compared to the remaining bell tower. The abrupt change in the plan section may be responsible for the non-uniform distribution of vertical stresses on the masonry below. Furthermore, as shown in Figure 3, the tower is configured as the juxtaposition of two hollow sections, whose connection is far from perfect. This, together with the possible presence of settlements, out-of-plumb and past horizontal forces, may explain the detachment of the south façade from the north part.

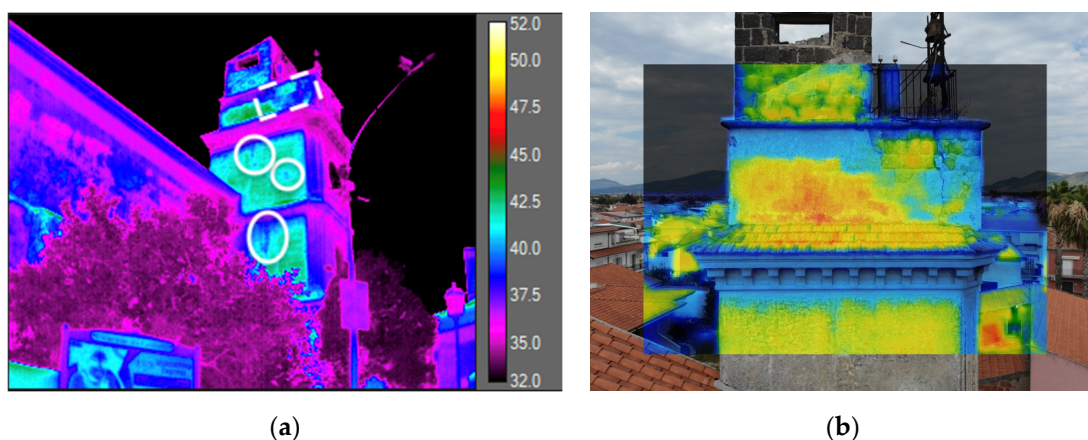


Figure 4. Cracking phenomenon observed on the west façade: inspection with thermal imager from ground (a) and with drone (b). Cracks are circled in white.

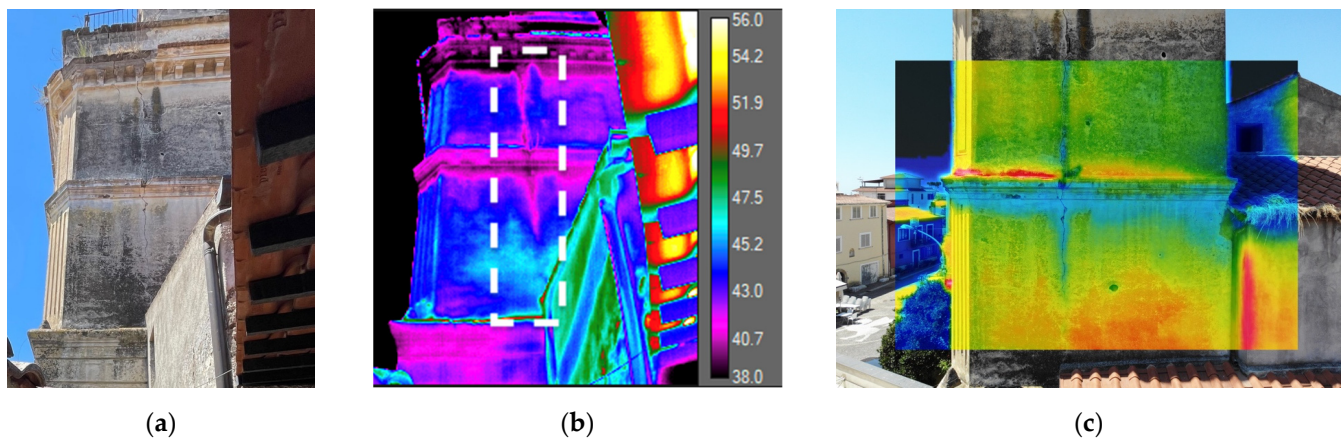


Figure 5. Cracking phenomenon observed on the east façade: (a) photo of the external wall and inspection with thermal imager from ground (b) and with drone (c). The vertical crack is highlighted in white.

3. Dynamical Identification

An Ambient Vibration Testing program was carried out on the tower to investigate the dynamical behavior under environmental sources. This approach is largely used to investigate the dynamical behavior of masonry bell towers [19,20]. The experimental setup consisted of 4 triaxial and 2 biaxial force-balanced accelerometers, with 2.5 V/g sensitivity and bandwidth 0–200 Hz, range $\pm 2g$, damping 0.707. The triaxial sensors were kept in the same position in all stages of the test: two sensors (T2, T3) were placed at 8.75 m height and the remaining two (T1 and T4) were placed at 12.25 m height (Figure 6). The biaxial sensors (B5, B6) were alternately placed at 5.25 m (setup I) and 8.75 m (setup II), and 15.00 and 17.80 m, respectively (setup III). This multi-setup testing program allowed for the estimation of the modal shapes along the height of the tower, according to the procedure shown in the following and implemented with in-house software developed at the University of Campania “Luigi Vanvitelli”.

Each setup acquisition lasted 900 s; the first setup was taken at 200 Hz sampling frequency, while setups II and III were applied at 100 Hz to reduce the amount of data. All signals were then corrected to zero average and decimation was applied up to a Nyquist frequency equal to 25 Hz (double decimation for setup I, single decimation for setup II and III).

The Fast Fourier Transforms (FFTs) of the signals (Figure 7) consistently show two peaks in two orthogonal directions at about 2.6 Hz and 3.1 Hz. Another lower peak is also recognized for some signals at about 5.9 Hz, while strong power density is also observed for accelerometer B6 in setup III for many frequencies between 6 and 12 Hz. Since this sensor was placed on the top of a wall not significantly constrained out of its plane (Figure 6), it seems clear that these frequencies are related to local modes of the top floor walls.

Frequencies and mode shapes were obtained by means of Frequency Domain Decomposition (FDD) [21], applying the procedure proposed by Amador and Brincker [22] to merge multiple setups having reference and roving sensors. In Figure 8, the first singular value (SVD 1) of the merged signals is plotted against frequencies. Three clear peaks are recognizable at 2.59 Hz, 3.08 Hz and 4.15 Hz. Some help in recognizing real modes when using FDD is offered by the analysis of the Modal Complexity Factor (MCF) for a given mode shape ψ_r , defined as in [23]

$$MCF = 1 - \frac{(S_{xx} - S_{yy})^2 + 4S_{xy}^2}{(S_{xx} + S_{yy})^2} \quad (1)$$

where

$$S_{xx} = Re\{\psi_r\}^T Re\{\psi_r\}, S_{yy} = Im\{\psi_r\}^T Im\{\psi_r\}, S_{xy} = Re\{\psi_r\}^T Im\{\psi_r\} \quad (2)$$

The MCF is a measure of how complex a mode is, and ranges from 0 (real mode) to 1 (imaginary mode). Since at each frequency f of the SVD plot it is possible to estimate a corresponding modal shape $\psi_r(f)$, $MCF(\psi_r)$ can be seen as a function of f . In Figure 8, the value $1-MCF(f)$ is plotted at each frequency level: it is possible to see that the maximum values of $1-MCF$, i.e., real modes, are observed corresponding to the SVD peaks. Real modes are also observed at two additional frequencies equal to 5.81 Hz and 6.15 Hz where PSD peaks are not evident. Thanks to this approach, these additional modal shapes and frequencies can be identified as modes of the structure.

The five identified modes are depicted in Figure 9. While the first two modes are translational modes, mainly along the two principal directions, with little effect of the interaction with the church, the fourth mode rather clearly appears as a torsional mode. Interestingly, similarities between modes 2 and 3 (translational along x), and 4 and 5 (torsional), respectively, seem to emerge from the analysis of the modal shapes and associated Modal Assurance Criterion (MAC) value (Figure 10). The presence of two modes of the same type at different frequencies, according to the authors, can only be explained by the alteration in the dynamical behavior generated by the physical discontinuity represented by the vertical crack observed in the two parallel walls (Figures 4 and 5).

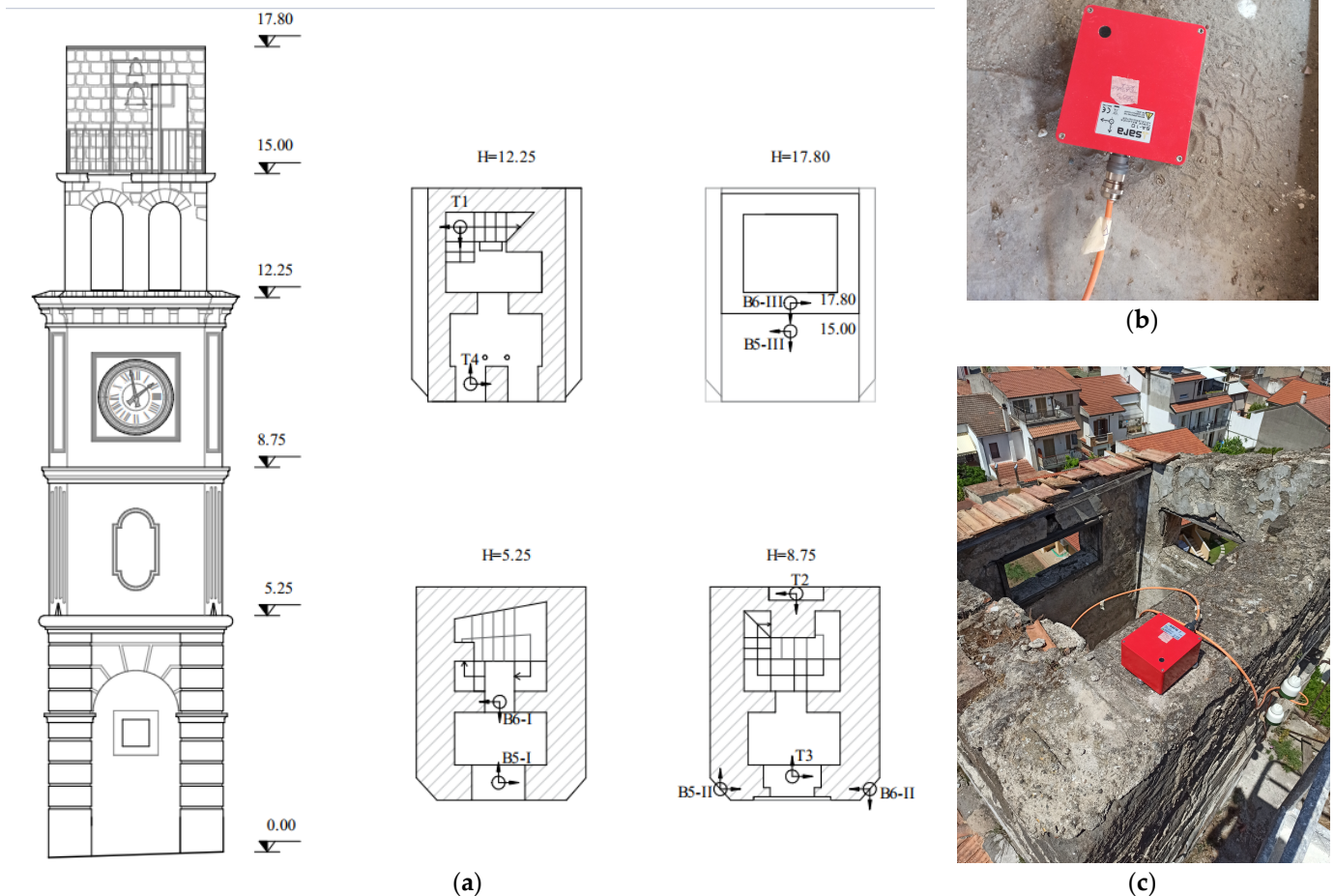


Figure 6. AVT setups: (a) position of the accelerometers, labelled as T (triaxial) or B (biaxial), with the Roman letter indicating the setup number; (b) view of T1 and (c) B6-III.

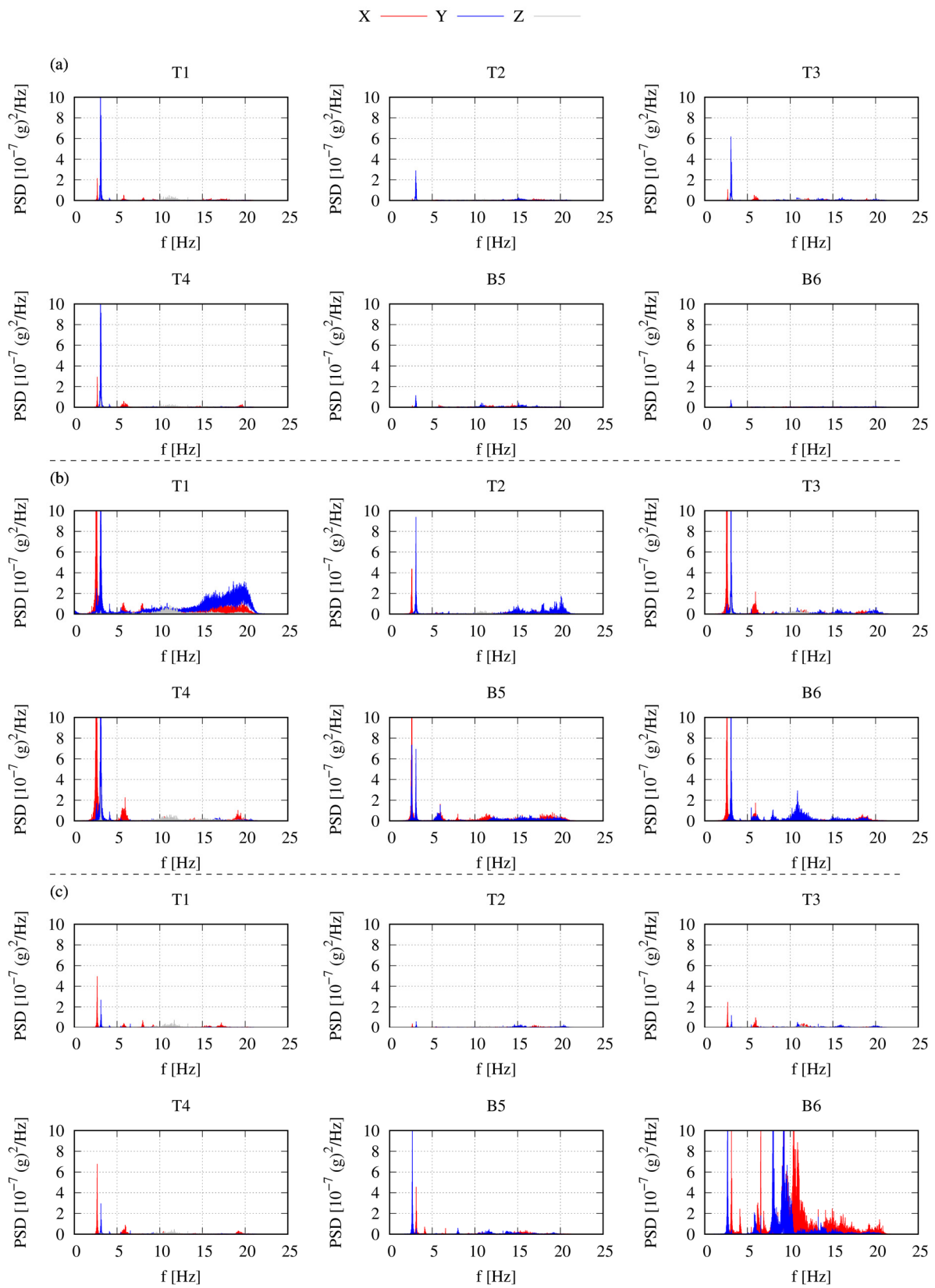


Figure 7. Fast Fourier Transform of the signals in the three directions: (a) setup I, (b) setup II and (c) setup III.

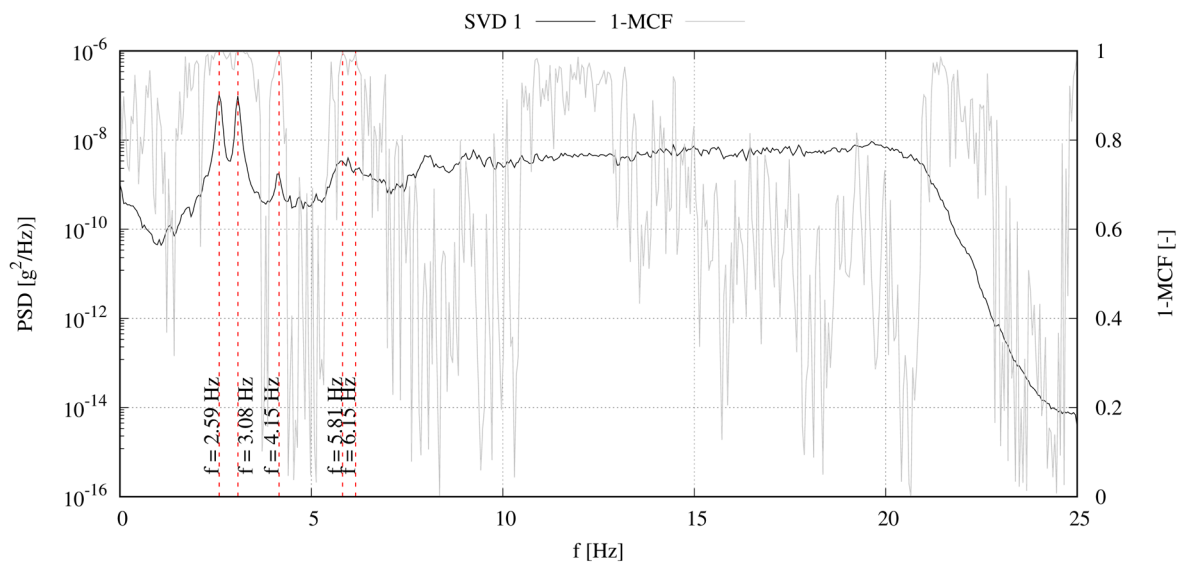


Figure 8. First Singular Value plot and identification of the first five frequencies.

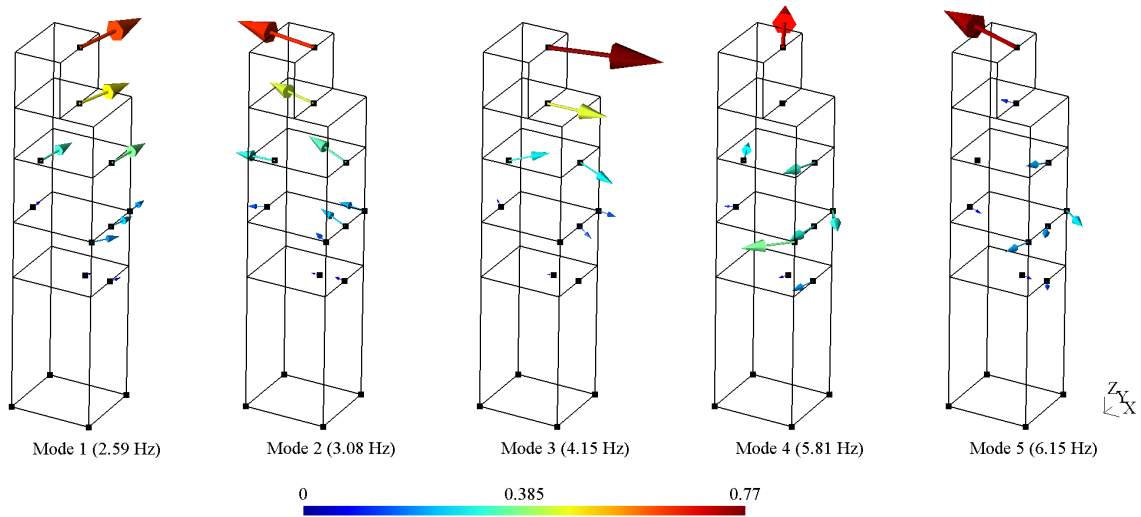


Figure 9. Identified modes of the bell tower.

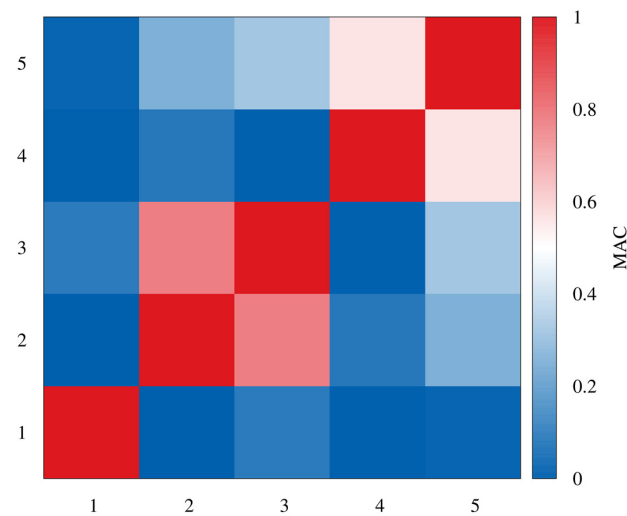


Figure 10. MAC table of the identified modes.

4. Seismic Assessment

4.1. Methodology

The observations collected during the survey and testing phases have direct consequences for the most suitable analysis approaches to use in the safety assessment. Firstly, the very low compressive strength detected through experimental testing directly leads to EL1 approach, where compression strength is the only significant material property. In addition, the significant cracking pattern observed in the tower makes it paramount to investigate the influence of local mechanisms and out-of-plane collapse modes on the safety of the bell tower, i.e., to use EL2 methodologies. Conversely, the use of sophisticated modeling approaches such as Finite Element Modeling (EL3) does not appear fully justified for two main reasons. On one hand, previous research [24] has clearly shown that the use of detailed material models that include softening and damage evolution may provide unreliable results if not coupled with extensive material characterization estimating less understood parameters, e.g., tensile strength, fracture energy, dilatancy parameters, etc., which is very difficult to perform in situ. On the other hand, the presence of pre-existing damage in the structure poses extraordinary challenges, especially in the context of macroscale modeling of masonry structures, and no established methods are available in the literature yet to determine realistically the effect of this damage on the final capacity. For all these reasons, lower detail levels (i.e., EL1 and EL2) were considered more suitable in this work to estimate the seismic vulnerability of the case under study.

In particular, according to EL1 approach, the tower is considered as a cantilever, variable-cross-section member subjected to its own weight, as well as a system of horizontal forces generated by the earthquake, assumed proportional to mass and height (linear acceleration profile). In addition to this code-compliant force system, a second one with accelerations proportional to the experimental mode shapes has been considered in this work. The collapse is due to combined compression and bending in a generic section, which provoke masonry crushing in the compressed area, as a result of partialization caused by the lack of tensile strength.

In the EL2 methodology, conversely, the seismic safety of the structure is evaluated by determining the ground acceleration that transforms the entire structure, or its significant individual parts (i.e., macro-elements), into a mechanism. This assessment can be conducted through linear kinematic analysis. The application of this method requires the analysis of the local mechanisms considered significant for the structure. These can be hypothesized based on the knowledge of the seismic behavior of and damage to similar structures, as observed in previous earthquakes or identified by the presence of specific crack patterns, even if non-seismic in nature. Additionally, in studying the local mechanisms, other aspects must also be considered: the quality of the connection between the masonry walls, the texture and arrangement of the masonry, the presence and efficiency of tie rods, the interactions with other structural elements or adjacent buildings, and phases of transformation that may be identifiable through construction details (e.g., heterogeneity of the masonry, juxtaposition of different types of walls, etc.).

4.2. EL1 Assessment

According to EL1 methodology, the structural check against combined compression and bending in a generic section is performed under the following hypotheses:

- conservation of plane sections;
- zero tensile strength of masonry;
- distribution of compressive forces according to a stress-block model.

The structural check is carried out along the two principal directions of inertia of the section, in both directions, and at different heights, considering the roof only as a superimposed load. The design moment can be evaluated by considering a system of forces distributed along the height of the structure, assuming either a linear or a mode-

proportional acceleration profile. The force to be applied at the centroid of each block is given by

$$F_i = \frac{W_i \cdot \zeta_i}{\sum_{k=1}^n W_k \cdot \zeta_k} F_h \tag{3}$$

where the following apply:

- F_h is the total shear base determined according to Equation (4);
- W_i and W_k are the weights of sectors i and k , respectively;
- $\zeta_i = z_i|\hat{\phi}_i$ is either z_i the height of the centroid of sector i with respect to the foundations (linear acceleration profile) or $\hat{\phi}_i$ the normalized modal displacements at the centroid along the considered principal direction (mode-proportional acceleration profile).

$$F_h = \frac{0.85 \cdot S_e(T_1) \cdot S \cdot W}{q \cdot g} \tag{4}$$

In Equation (4), the following apply:

- $S_e(T_1)$ is the ordinate of the elastic response spectrum, a function of the first period T_1 of the structure in the considered direction;
- S is the amplification factor due to soil and topographic conditions;
- W is the total weight of the tower;
- q is the behavior factor;
- g is the gravity acceleration.

The resultant of the seismic forces F_{hi} acting on the i -th section is given by Equation (5), while the relative height z_{Fi} at which F_{hi} is applied is calculated as per Equation (6).

$$F_{hi} = \frac{\sum_{k=i}^n W_k \zeta_k}{\sum_{k=1}^n W_k \zeta_k} F_h \tag{5}$$

$$z_{Fi} = \frac{\sum_{k=i}^n W_k \zeta_k z_k}{\sum_{k=i}^n W_k \zeta_k} - z_i^* \tag{6}$$

where in the above equations z_i^* is the height of the i -th verification section relative to the base.

By imposing the equality between the resisting bending moment $M_{u,i}$ and the design bending moment $M_{ed,i}$:

$$M_{u,i} = F_{hi} z_{Fi} \tag{7}$$

it is possible to derive the value of the ordinate of the elastic response spectrum corresponding to the achievement of the Ultimate Limit State (ULS) in the i -th section (taking into account the confidence factor F_C):

$$S_{e,ULS,i}(T_1) = \frac{q \cdot g \cdot M_{u,i} \sum_{k=1}^n W_k \zeta_k}{0.85 W (\sum_{k=i}^n W_k \zeta_k z_k - z_i^* \sum_{k=i}^n W_k \zeta_k) F_C} \tag{8}$$

Based on this value, the corresponding Peak Ground Acceleration (PGA) a_{ULS} is evaluated by considering the parameters of the design spectrum at the ULS and the fundamental period of the structure.

In cases of hollow rectangular sections, such as the ones typical of the tower under consideration, the ultimate moment of resistance at the base of the i -th sector can be calculated as per Equation (9):

$$M_{u,i} = \frac{\sigma_{0i} A_i}{2} \left(b_i - \frac{\sigma_{0i} A_i}{0.85 a_i f_d} \right) \tag{9}$$

where the following apply:

- a_i is the length of the side perpendicular to the direction of the considered seismic action for the i -th section, excluding any openings;
- b_i is the length of the side parallel to the direction of the considered seismic action for the section under analysis;
- A_i is the total area of the section under analysis, excluding any openings;
- σ_{0i} is the average normal stress in the section under analysis (W/A_i , where W is the weight of the structure above the section under analysis);
- f_d is the design compressive strength of the masonry.

Next, it is possible to calculate the acceleration factor $f_{a,ULS}$ as the ratio between the collapse acceleration and the maximum expected peak ground acceleration at the site ($a_{g,ULS}$):

$$f_{a,ULS} = \frac{a_{ULS}}{a_{g,ULS}} \quad (10)$$

Given the exposure characteristics of the tower (nominal life of 50 years and use class III), the return period of the seismic action at the Ultimate Limit State is assumed to be 712 years. The elastic response spectrum (ULS) adopted for the EL1 structural check is shown in Figure 11 (soil type C, flat soil), and it is characterized by $a_{g,ULS} = 0.103$ g.

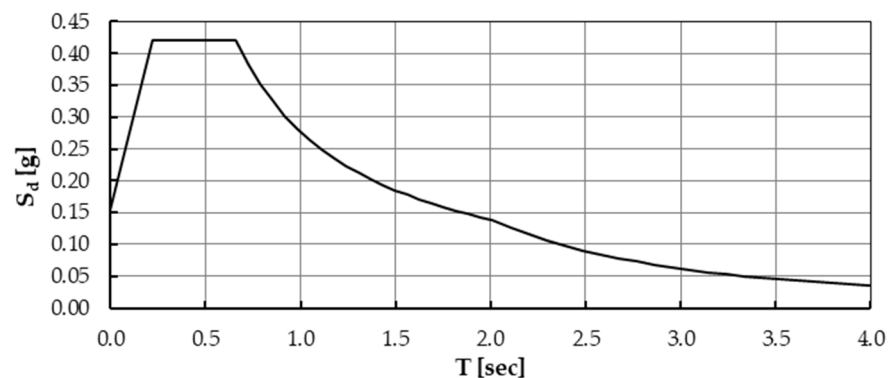


Figure 11. Elastic response spectrum for EL1 analysis.

The fundamental period (T_1) was determined according to the AVT results. In this sense, it should be remarked that both first and second vibration periods (0.39 s and 0.32 s, respectively), which correspond to translational modes in the two principal directions of the tower, are included in the constant branch of the design response spectrum.

In the presence of limited tests on materials, the Italian code [25] suggests a procedure that, starting from some typology-based ranges for mechanical properties, updates their median values accounting for the results of the tests. Applying this methodology to the type of masonry under consideration, an average compressive strength $f_m = 1.23$ MPa was obtained. Nonetheless, given that the tests consistently returned lower compressive strength values, in the next calculation, $f_m = 0.7$ MPa was assumed, based on the results obtained from the sclerometer, double flat jack test and compressive test on masonry sample. This value was then reduced due to the partial safety factor for masonry for seismic actions ($\gamma_M = 2.0$) and a confidence factor $F_C = 1.20$, with the latter defined according to the performed investigation activity. Thus, $f_d = 0.29$ MPa was adopted.

As specified in equation (3), both a linear displacement and mode-proportional force distributions along the height of the bell tower were considered. The mode-proportional distributions were defined according to the AVT results. In particular, the profiles of normalized modal displacements ($\hat{\varphi} = \varphi_i / \varphi_{max}$) related to the 1st (y-direction) and 2nd (x-direction) vibrational modes shown in Figure 12 were adopted.

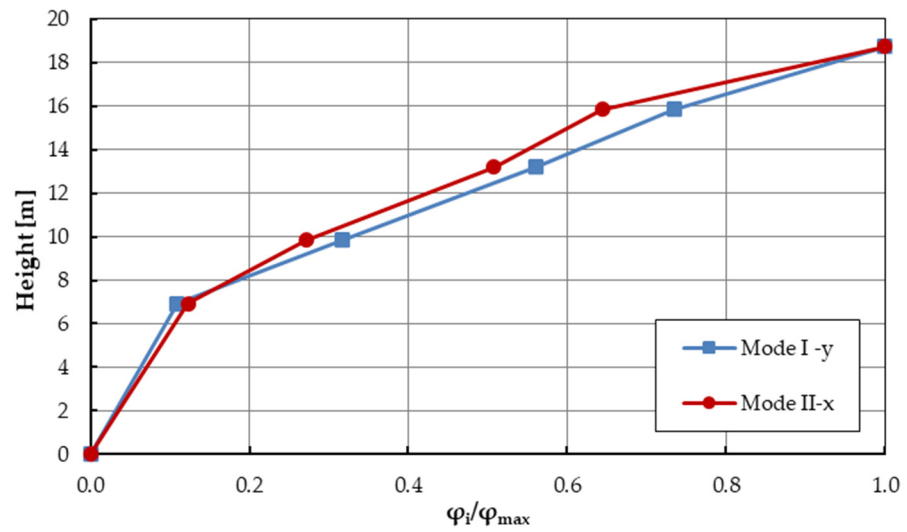


Figure 12. Normalized mode-proportional displacement profiles adopted for the EL1 checks.

For the EL1 analysis, the tower was thus divided into sectors, whose base sections were considered for the structural checks, according to the scheme proposed in Figure 13.

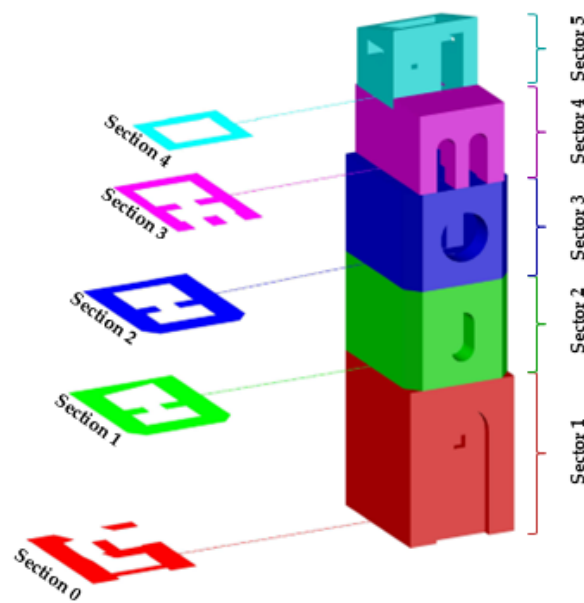


Figure 13. Subdivision of the tower in sectors and sections adopted for the EL1 checks.

The seismic weight of each sector was estimated by assuming a density of the masonry $\gamma = 1600 \text{ kg/m}^3$, as returned by laboratory tests. The summary of the weight estimation is reported in Table 1.

Table 1. Seismic weight estimation.

Sector	Volume [m ³]	z _k (m)	γ (kg/m ³)	W _k (kN)
1	43.12	2.63	1600	620.9
2	38.85	7.00	1600	559.4
3	33.87	10.46	1600	487.7
4	20.56	13.61	1600	296.1
5	10.21	16.20	1600	147.0

Based on the total weight of the tower ($W = 2111.18$ kN), the base shear F_h was determined by assuming $S = 1.5$ (due to the soil type and topographic conditions) and a behavior factor $q = 2.8$, according to the minimum value of the range proposed in [4]. The calculation returned $F_h = 269$ kN.

Thus, the seismic forces to be applied at the centroid of each tower sector were determined according to equation (3). The results are shown in Tables 2 and 3 for the linear displacement and mode-proportional acceleration profiles, respectively.

Table 2. Estimation of seismic forces (linear acceleration profile).

Sector	z_k (m)	W_k (kN)	$z_k \cdot W_k / \sum(z_k \cdot W_k)$ (-)	F_i (kN)
5	16.20	163.36	0.140	37.6
4	13.61	328.96	0.236	63.6
3	10.46	669.92	0.299	80.6
2	7.00	653.60	0.230	61.8
1	2.63	935.68	0.096	25.8

Table 3. Estimation of seismic forces (mode-proportional acceleration profiles).

Sector	$\hat{\phi}_i$ (1st Mode-y)	$\hat{\phi}_i$ (2nd Mode-x)	W_k [kN]	$\hat{\phi}_i \cdot W_i / \sum(\hat{\phi}_k \cdot W_k)$ (1st Mode-y)	$\hat{\phi}_i \cdot W_i / \sum(\hat{\phi}_k \cdot W_k)$ (2nd Mode-x)	$F_{i,y}$ [kN]	$F_{i,x}$ [kN]
5	0.77	0.69	163.36	0.204	0.198	55.0	53.3
4	0.59	0.53	328.96	0.315	0.307	84.9	82.7
3	0.36	0.31	669.92	0.319	0.300	85.9	80.9
2	0.11	0.13	653.60	0.115	0.138	31.0	37.3
1	0.04	0.05	935.68	0.047	0.057	12.5	15.3

By applying the procedure above described, it was possible to estimate the acting bending moments at the base of each sector of the tower and compare them with the bending capacities (determined as the minimum among both positive and negative along the two directions). The results in terms of minimum acceleration factors $f_{a,ULS}$ for each sector obtained with a linear acceleration profile are summarized in Table 4, while in Figure 14 the comparison among acting and resisting bending moments for the two principal directions is graphically shown. Similarly, the results obtained by assuming mode-proportional acceleration profiles are summarized in Tables 5 and 6 for 1st and 2nd modes, respectively—and shown in Figure 15.

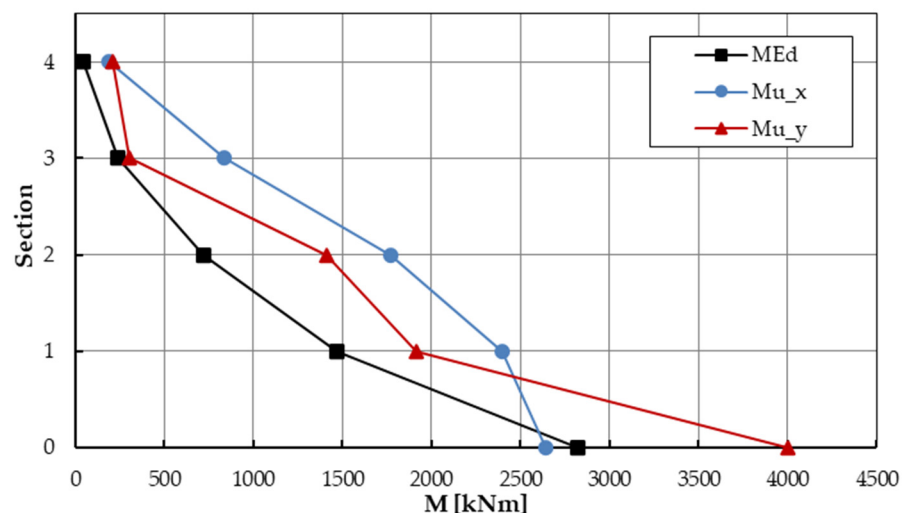


Figure 14. Comparison between design and resisting bending moments at each relevant section (linear acceleration profile).

Table 4. Structural check of relevant sections according to EL1 procedure (linear acceleration profile).

Section	z_i^* (m)	$M_{ed,i}$ (kNm)	$M_{u,i}$ (kNm)	$S_{e,ULS,i}$ (m/s ²)	$a_{ULS,i}$ (m/s ²)	$f_{a,ULS}$ (-)
0	0.00	2818.7	2639.9	3.86	0.95	0.94
1	5.26	1469.3	1911.3	5.36	1.31	1.30
2	8.77	723.6	1413.1	8.05	1.97	1.95
3	12.25	235.1	302.8	5.31	1.30	1.29
4	15.00	45.1	184.4	16.85	4.13	4.09

Table 5. Structural check of relevant sections according to EL1 procedure (1st mode-proportional).

Section	$M_{edy,i}$ [kNm]	$M_{uy,i}$ [kNm]	$S_{e,ULS,i}$ [m/s ²]	$a_{ULS,i}$ [m/s ²]	$f_{a,ULS}$ [-]
0	3196.15	4002.7	5.16	1.27	1.25
1	1811.95	1911.3	4.35	1.07	1.05
2	965.13	1413.1	6.04	1.48	1.46
3	332.85	302.8	3.75	0.92	0.91
4	66.03	211.7	13.23	3.24	3.21

Table 6. Structural check of relevant sections according to EL1 procedure (2nd mode-proportional).

Section	$M_{edx,i}$ [kNm]	$M_{ux,i}$ [kNm]	$S_{e,ULS,i}$ [m/s ²]	$a_{ULS,i}$ [m/s ²]	$f_{a,ULS}$ [-]
0	3135.84	2639.9	3.47	0.85	0.84
1	1758.90	2396.6	5.62	1.38	1.36
2	932.92	1771.9	7.83	1.92	1.90
3	323.05	833.6	10.64	2.61	2.58
4	63.99	184.4	11.89	2.91	2.88

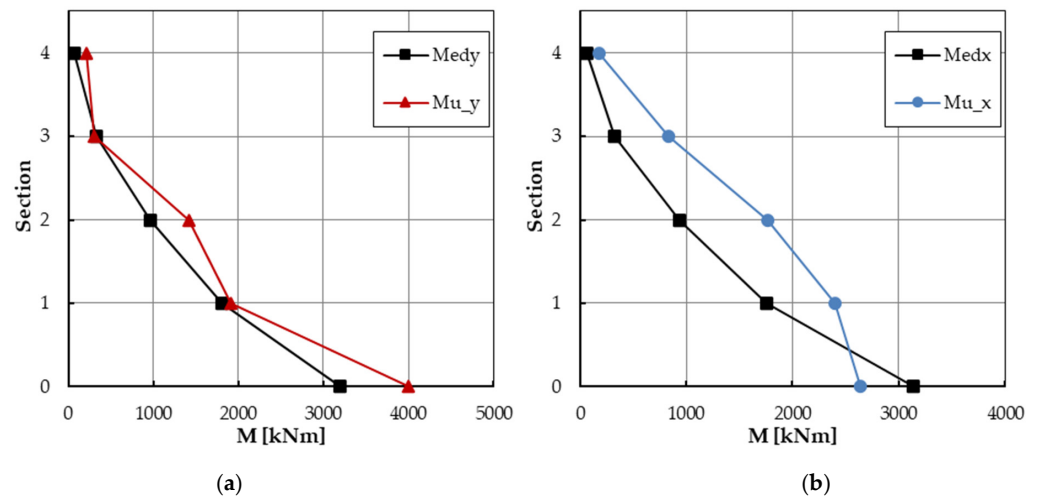


Figure 15. Comparison between design and resisting bending moment at each relevant section: (a) 1st mode-proportional and (b) 2nd mode proportional acceleration profiles.

According to EL1 methodology, which allows for performing a simplified structural check neglecting out-of-plane and shear failures, the bell tower under investigation presents a safety factor of less than unity for design seismic loads at the ULS, and thus cannot be considered safe. In particular, by assuming a linear displacement and 2nd mode proportional load distributions (along x-direction), the base section returned a safety index in terms of acceleration equal to 0.94 and 0.84, respectively. On the other hand, when a 1st mode proportional load pattern was considered, the section at the base of the 3rd sector was the sole returning a negative outcome of the structural checks. This can be related to

the significant openings the tower presents at this level. In the other cases, the analyzed sections were verified with a safety index in terms of acceleration ranging from 1.05 (section 1, 1st mode proportional) and 4.09 (section 4, linear distribution).

It must be pointed out that the above calculations were performed by rigorously following the prescriptions reported in [4]. With reference to the behavior factor, past studies demonstrated that the assumption of q between 2.8 (for towers with abrupt changes in stiffness along the height or for bounded towers) to 3.6 (for structures that are regular in elevation), which is derived from the extrapolation of values for palaces and buildings, is possibly overestimated due to the lack of structural redundancy of the bell tower static scheme [11,12,16]. Moreover, the behavior factor is intended as a synthetic index about the capacity of a structure to dissipate energy due to ductile behavior, and it should also be related to the actual stress rate of the material under permanent load conditions. Based on this, and given the very poor quality of the masonry at hand, the calculations were performed again by considering non-dissipative behavior of the tower ($q = 1.5$). This led to a reduction in the acceleration factors $f_{a,ULS}$ reported in Tables 4–6 by a coefficient of 1.87 (i.e., $2.8/1.5$), which, thus, under this assumption, ranges between 0.45 (section 1, 2nd mode-proportional profile) and 2.19 (section 4, linear profile), with most of the relevant sections having an unsatisfactory safety check. The new comparison among acting and resisting bending moments for the two principal directions is graphically shown in Figures 16 and 17, for linear and mode-proportional acceleration profiles, respectively.

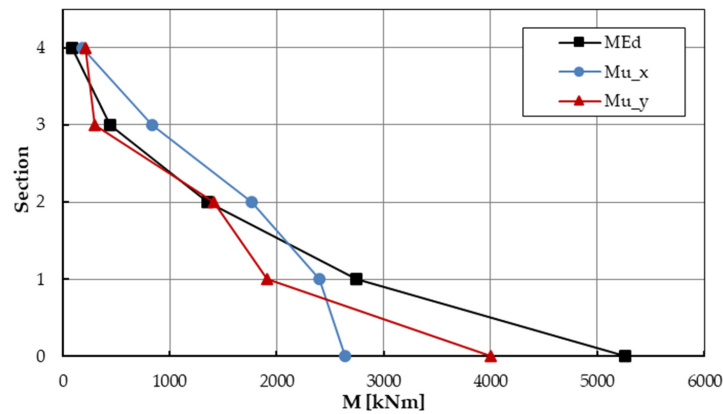


Figure 16. Comparison between design and resisting bending moment at each relevant section, with $q = 1.5$ (linear acceleration profile).

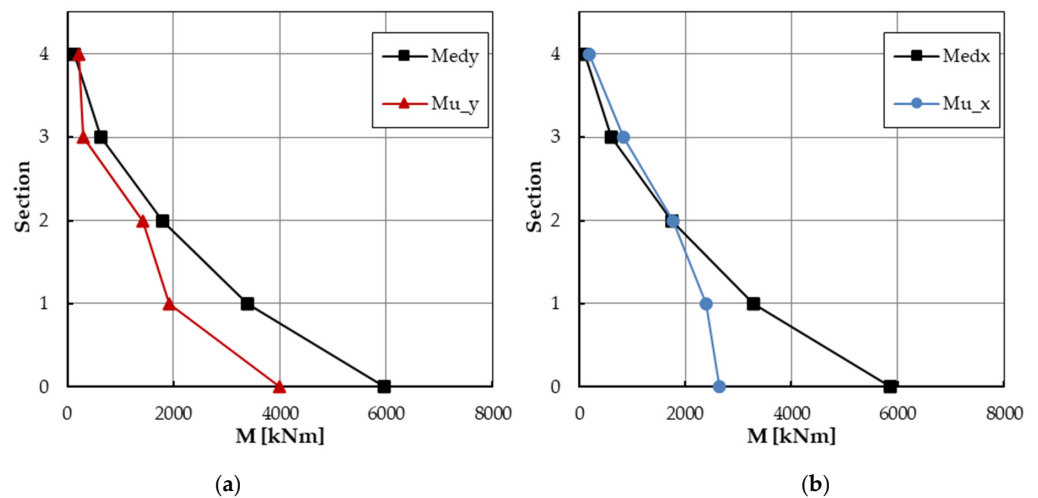


Figure 17. Comparison between design and resisting bending moment at each relevant section with $q = 1.5$: (a) 1st mode-proportional and (b) 2nd mode-proportional acceleration profiles.

4.3. EL2 Assessment

In order to estimate the load multiplier α_0 provoking the activation of the local damage mechanism according to the EL2 methodology, the following forces acting on the rigid blocks of the kinematic chain must be considered:

- the self-weight of the blocks applied at their centroid and other carried vertical loads (self-weight and superimposed loads from floors and roofing, and other masonry elements not considered in the structural model);
- horizontal forces proportional to the carried vertical loads, if these are not effectively transferred to other parts of the building;
- any external forces (e.g., those transmitted by tie roads);
- any internal forces (e.g., actions related to the interlocking between masonry blocks).

Given a virtual rotation to the generic k block, based on the geometry of the structure, the displacements related to each considered load are calculated. Thus, by applying the Principle of Virtual Works, the value of α_0 can be calculated according to Equation (11):

$$\alpha_0 \left(\sum_{i=1}^n P_i \cdot \delta_{x,i} + \sum_{j=n+1}^{n+m} P_j \cdot \delta_{x,j} \right) - \sum_{i=1}^n P_i \cdot \delta_{y,i} + \sum_{k=1}^o F_k \cdot \delta_k = L_{fi} \quad (11)$$

where the following apply:

- n is the number of all weight forces P_i applied at the centroid of the different blocks of the kinematic chain;
- m is the number of weight forces P_j not directly acting on the blocks, whose masses generate horizontal forces on the elements of the kinematic chain due to the seismic action, as they are not effectively transferred to other parts of the building;
- o is the number of external forces F_k , not associated with masses, applied to the various blocks;
- $\delta_{x,i}$ (resp. $\delta_{y,i}$) is the virtual horizontal (resp. vertical) displacement of the point of application of the i -th weight P_i , assuming the positive direction as the seismic action activating the mechanism acts (resp. upward);
- δ_k is the virtual displacement of the point where the h -th external force is applied parallel to and with the same sign as the force;
- L_{fi} is the work of the internal forces.

To perform the safety checks, the horizontal multiplier α_0 activating the mechanism is transformed into spectral acceleration a_0^* according to Equation (12), in order to have consistency with the demand measure.

$$a_0^* = \frac{\alpha_0 \cdot g}{e^* F_c} \quad (12)$$

In Equation (12), e^* is the portion of the participating mass in the considered mechanism, which is estimated according to Equation (13).

$$e^* = \frac{(\sum_{i=1}^{n+m} P_i \cdot \delta_{x,i})^2}{\sum_{i=1}^{n+m} P_i \cdot \sum_{i=1}^{n+m} (P_i \cdot \delta_{x,i}^2)} \quad (13)$$

If the considered collapse mechanism includes an isolated element or a portion of the construction supported on the ground, the safety check (ULS) is fulfilled if the spectral acceleration a_0^* satisfies the following condition:

$$q \cdot a_0^* \geq a_{g,ULS} \cdot S \quad (14)$$

where S is the amplification due to the soil conditions (1.5 for the case under consideration) and the behavior factor is assumed as $q = 2.0$ [25].

Conversely, if the local mechanism affects a portion of the building located at a certain height, it is necessary to account for amplifying effects according to Equation (15):

$$q \cdot a_0^* \geq S_e(T_1) \cdot \psi(Z) \cdot \gamma \quad (15)$$

where the following apply:

- $\psi(Z)$ is the first mode of vibration in the considered direction, normalized to one at the top of the building (in the absence of more accurate assessments, $\psi(Z) = Z/H$, with H the height of the structure relative to the foundation);
- Z is the height, relative to the foundation of the building, of the centroid of the boundary lines between the blocks affected by the mechanism and the rest of the structure;
- γ is the corresponding modal participation factor, equal to $3N/(2N + 1)$.

The described procedure was adopted by considering four collapse mechanisms, defined according to typical failure modes of masonry towers and the observed cracking phenomena. In particular, the following were considered:

1. overturning of the portion of sector 4 due to the presence of vertical cracks (Figure 18a);
2. overturning of the portion of sectors 3 and 4 due to the presence of vertical cracks (Figure 18b);
3. overturning of the last sector of the tower characterized by different material features (Figure 18c);
4. overturning of sectors 4 and 5 due to the presence of vertical cracks (Figure 18d).

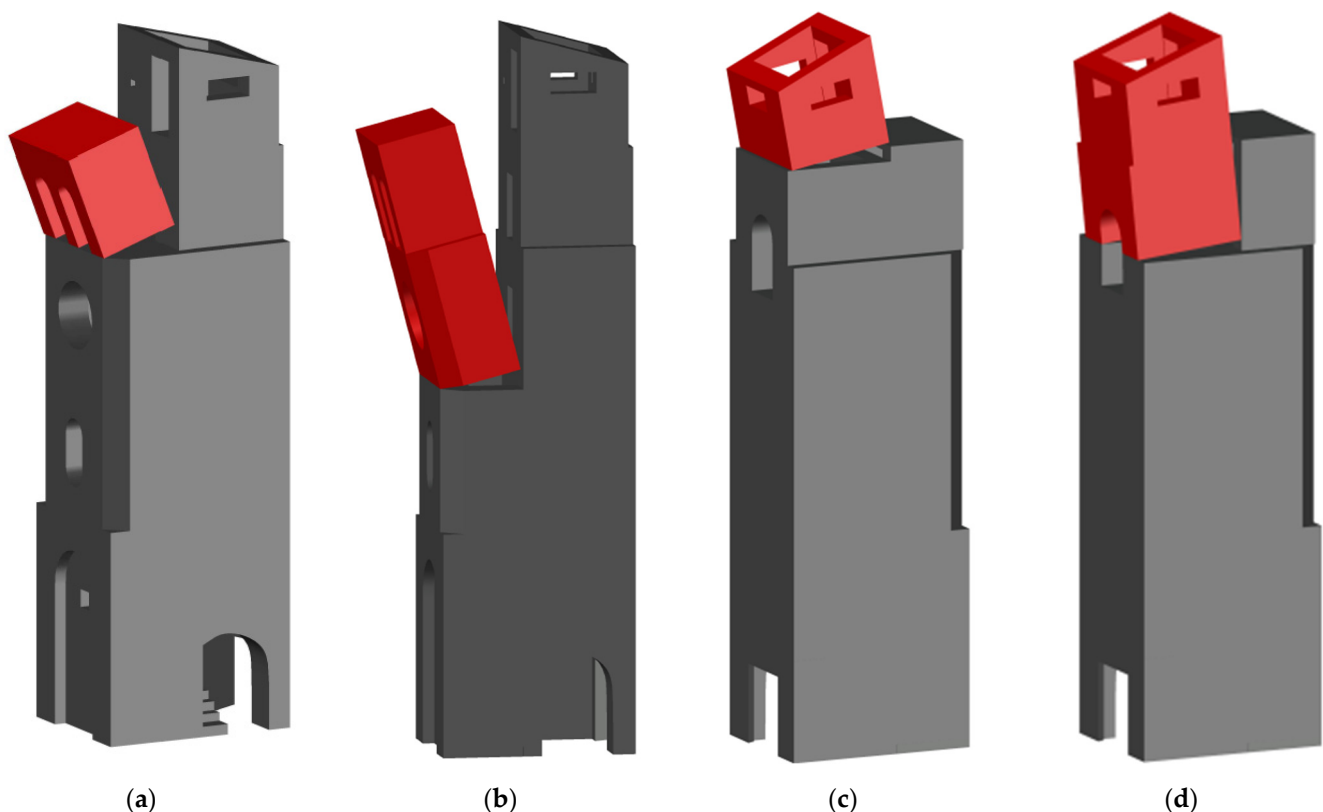


Figure 18. The considered collapse mechanisms for the EL2 assessment: (a) overturning of part of sector 4, (b) overturning of part of sectors 3 and 4, (c) overturning of sector 5, (d) overturning of sectors 4 and 5.

Again, the structural checks were performed by providing the acceleration factor, $f_{a,ULS}$ defined as per Equation (10). The EL2 assessment results are summarized in Table 7.

Table 7. Structural check of collapse mechanisms relevant to EL2 procedure.

Mechanism	$Se(T1)\psi(Z)\gamma/q$ (m/s ²)	a_0^* (m/s ²)	$f_{a,ULS}$ (-)
1	1.94	1.15	0.59
2	1.39	1.96	1.41
3	2.37	11.92	5.02
4	1.94	4.00	2.06

The results show that the minimum value of the safety index in terms of acceleration is 0.59. This minimum safety index value is associated with the collapse mechanism 1 of the masonry section in sector 4, which, in its current state (characterized by cracks where it connects with the remaining part of the masonry in the sector), behaves like a monolithic wall. The other mechanisms considered returned positive outcomes, with safety indexes in the range of 1.41 (mechanism 2) to about 5 (mechanism 3).

5. Conclusions

In this paper, the safety vulnerability assessment of a historical masonry bell tower is described. In a first phase, a detailed survey was carried out by means of internal and external laser-scanning, thermography and visual inspection. Subsequently, materials were characterized through non- and semi-destructive testing, including sclerometer and penetrometer tests, single and double flat-jacks and tests on stone cores. The outcome of this phase was the picture of a structure made of low-quality materials and characterized by extensive cracking particularly vertically on the external walls.

To characterize the global dynamic behavior, AVTs were performed. The results, post-processed using Frequency Domain Decomposition enhanced by the examination of the Modal Complexity Factor, indicated fundamental frequencies ranging in the constant branch of the design spectrum, and, more interestingly, the presence of similar modes associated with well separated frequencies. This was explained as a result of the physical separation of the structure due to the presence of the vertical cracks, thus indicating a significant effect of the damage state on the dynamic behavior.

Motivated by these results, the final vulnerability assessment was carried out by means of EL1 and EL2 methodologies. Both approaches provided safety factors less than unity, thus indicating the need for seismic retrofitting. In particular, in the case of the EL1 approach the bottom section failure was estimated at a PGA less than that corresponding to the design spectrum at the Ultimate Limit State, as well as considering, in the authors' view, the rather optimistic behavior factor $q = 2.8$. In the case of EL2, a mechanism triggered by the observed vertical cracks provided activation ground acceleration equal to less than 60% of the design PGA at the ULS.

This paper shows the information that can be obtained from documental research survey and experimental activities with the aim of vulnerability assessment of historical masonry towers. It also points out some limitations of current practice that need to be investigated in the future, such as for instance a more realistic behavior factor estimation. Further research will focus on effective and compatible retrofitting actions for the specific bell tower; more generally, embedding pre-existing damage in a detailed modeling framework will also be investigated, as this represents an important topic with critical relevance in the application of detailed modeling to historical heritage.

Author Contributions: Conceptualization, C.C., M.Z., A.L. and G.D.M.; methodology, C.C., M.Z. and A.L.; software, C.C. and A.L.; validation, C.C., A.L. and M.Z.; investigation, C.C., A.L. and M.Z.; resources, G.D.M.; writing—original draft preparation, C.C. and M.Z.; writing—review and editing, C.C., M.Z., A.L. and G.D.M.; visualization, C.C. and M.Z.; supervision, G.D.M.; project administration, S.F. and G.D.M.; funding acquisition, G.D.M. All authors have read and agreed to the published version of the manuscript.

Funding: This research was funded by European Union-Next Generation EU, Mission 4 Component 1 through the project PRIN 2022 PNRR “SAFE_MOTION–Structural Assessment and development of innovative safeguard measures for historical masonry towers” (CUP B53D23027300001). M.Z. is funded by MUR (Ministry of University and Research) through PON FSE 2014-2020 program (contract: 49-I-32603-3).

Data Availability Statement: The raw data supporting the conclusions of this article will be made available by the authors on request.

Acknowledgments: The authors kindly acknowledge the technical support provided by Gianfranco Fiondella in the experimental activities and Marianna Donciglio during the analyses.

Conflicts of Interest: The authors declare no conflicts of interest. The funders had no role in the design of the study; in the collection, analyses, or interpretation of data; in the writing of the manuscript; or in the decision to publish the results.

References

1. Testa, F.; Barontini, A.; Chieffo, N.; Lourenço, P.B. Observed damage and simplified risk assessment of Italian masonry bell towers struck by past seismic events. *Bull. Earthq. Eng.* **2024**, *22*, 3353–3385. [[CrossRef](#)]
2. De Matteis, G.; Zizi, M. Seismic Damage Prediction of Masonry Churches by a PGA-based Approach. *Int. J. Archit. Herit.* **2019**, *13*, 1165–1179. [[CrossRef](#)]
3. Zizi, M.; Rouhi, J.; Chisari, C.; Cacace, D.; De Matteis, G. Seismic Vulnerability Assessment for Masonry Churches: An Overview on Existing Methodologies. *Buildings* **2021**, *11*, 588. [[CrossRef](#)]
4. Ministero per i Beni e le Attività Culturali. *Valutazione e riduzione del rischio sismico del patrimonio culturale con riferimento alle Norme tecniche per le costruzioni di cui al D.M. 14/01/2008*; Ministero per i Beni e le Attività Culturali: Roma, Italy, 2011.
5. Bartoli, G.; Betti, M.; Vignoli, A. A numerical study on seismic risk assessment of historic masonry towers: A case study in San Gimignano. *Bull. Earthq. Eng.* **2016**, *14*, 1475–1518. [[CrossRef](#)]
6. Lucchesi, M.; Pintucchi, B. A numerical model for non-linear dynamic analysis of slender masonry structures. *Eur. J. Mech. A/Solids* **2007**, *26*, 88–105. [[CrossRef](#)]
7. Torelli, G.; D’Ayala, D.; Betti, M.; Bartoli, G. Analytical and numerical seismic assessment of heritage masonry towers. *Bull. Earthq. Eng.* **2020**, *18*, 969–1008. [[CrossRef](#)]
8. D’Ayala, D.; Speranza, E. Definition of collapse mechanisms and seismic vulnerability of historic masonry buildings. *Earthq. Spectra* **2003**, *19*, 479–509. [[CrossRef](#)]
9. Bartoli, G.; Betti, M.; Galano, L.; Zini, G. Numerical insights on the seismic risk of confined masonry towers. *Eng. Struct.* **2019**, *180*, 713–727. [[CrossRef](#)]
10. Di Gennaro, L.; Guadagnuolo, M.; Monaco, M. Rocking Analysis of Towers Subjected to Horizontal Forces. *Buildings* **2023**, *13*, 762. [[CrossRef](#)]
11. Ceroni, F.; Pecce, M.; Manfredi, G. Seismic Assessment of the Bell Tower of Santa Maria Del Carmine: Problems and Solutions. *J. Earthq. Eng.* **2009**, *14*, 30–56. [[CrossRef](#)]
12. D’Ambrisi, A.; Mariani, V.; Mezzi, M. Seismic assessment of a historical masonry tower with nonlinear static and dynamic analyses tuned on ambient vibration tests. *Eng. Struct.* **2012**, *36*, 210–219. [[CrossRef](#)]
13. Ferraioli, M.; Lavino, A.; Abruzzese, D.; Avossa, A.M. Seismic Assessment, Repair and Strengthening of a Medieval Masonry Tower in Southern Italy. *Int. J. Civ. Eng.* **2020**, *18*, 967–994. [[CrossRef](#)]
14. Micelli, F.; Cascardi, A. Structural assessment and seismic analysis of a 14th century masonry tower. *Eng. Fail. Anal.* **2020**, *107*, 104198. [[CrossRef](#)]
15. Shehu, R. Preliminary Assessment of the Seismic Vulnerability of Three Inclined Bell-Towers in Ferrara, Italy. *Int. J. Archit. Herit.* **2020**, *in press*. [[CrossRef](#)]
16. Chisari, C.; Cacace, D.; De Matteis, G. A mechanics-based model for simplified seismic vulnerability assessment of masonry bell towers. *Eng. Struct.* **2022**, *270*, 114876. [[CrossRef](#)]
17. Shakya, M.; Varum, H.; Vicente, R.; Costa, A. Seismic vulnerability assessment methodology for slender masonry structures. *Int. J. Archit. Herit.* **2018**, *12*, 1297–1326. [[CrossRef](#)]
18. Sepe, V.; Speranza, E.; Viskovic, A. A method for large-scale vulnerability assessment of historic towers. *Struct. Control Health Monit.* **2008**, *15*, 389–415. [[CrossRef](#)]
19. Aloisio, A.; Capanna, I.; Cirella, R.; Alaggio, R.; Di Fabio, F.; Fragiaco, M. Identification and Model Update of the Dynamic Properties of the San Silvestro Belfry in L’Aquila and Estimation of Bell’s Dynamic Actions. *Appl. Sci.* **2020**, *10*, 4289. [[CrossRef](#)]
20. Erkek, H.; Calayir, Y.; Yetkin, M. Non-linear seismic behavior of historic Adana Great Clock Tower. *Structures* **2024**, *65*, 106704. [[CrossRef](#)]
21. Brincker, R.; Zhang, L.; Andersen, P. Modal identification of output-only systems using frequency domain decomposition. *Smart Mater. Struct.* **2001**, *10*, 441–445. [[CrossRef](#)]

22. Amador, S.D.R.; Brincker, R. Robust multi-dataset identification with frequency domain decomposition. *J. Sound Vib.* **2021**, *508*, 116207. [[CrossRef](#)]
23. Structural Vibration Solutions. Modal Complexity Factor. Available online: https://www.svibs.com/resources/ARTEMIS_Modal_Help_v7/Generic%20Complexity%20Plot.html (accessed on 26 September 2024).
24. Zizi, M.; Chisari, C.; Rouhi, J.; De Matteis, G. Comparative analysis on macroscale material models for the prediction of masonry in-plane behavior. *Bull. Earthq. Eng.* **2022**, *20*, 963–996. [[CrossRef](#)]
25. Ministero delle Infrastrutture e dei Trasporti. *Istruzioni per l'applicazione dell'«Aggiornamento delle “Norme tecniche per le costruzioni”» di cui al decreto ministeriale 17 gennaio 2018; CIRCOLARE 21 gennaio 2019, n. 7 C.S.LL.PP*; Ministero delle Infrastrutture e dei Trasporti: Roma, Italy, 2019.

Disclaimer/Publisher’s Note: The statements, opinions and data contained in all publications are solely those of the individual author(s) and contributor(s) and not of MDPI and/or the editor(s). MDPI and/or the editor(s) disclaim responsibility for any injury to people or property resulting from any ideas, methods, instructions or products referred to in the content.